AD-A146 640 STUDIES OF SIC FORMATION ON SI(100) BY CHEMICAL VAPOR DEPOSITION(U) PITTSBURGH UNIV PA SURFACE SCIENCE CENTER F BOZSO ET AL. SEP 84 3 1/1

UNCLASSIFIED F/G 20/1 NL

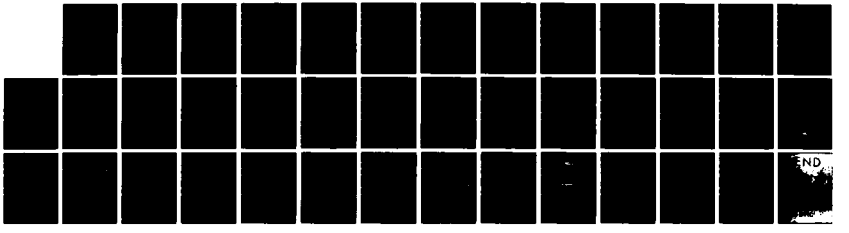

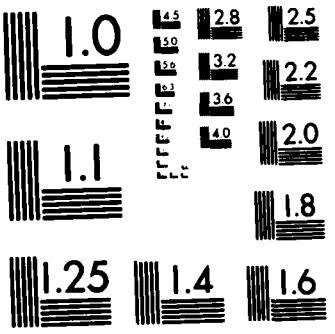

SECURITY CLASSIFICATION OF THIS PAGE (When Data Entered)

REPORT DOCUMENTATION PAGE		READ INSTRUCTIONS BEFORE COMPLETING FORM
1. REPORT NUMBER: 3	2. GOVT ACCESSION NO.	3. RECIPIENT'S CATALOG NUMBER
4. TITLE (and Subtitle): Studies of SiC Formation on Si(100) by Chemical Vapor Deposition		5. TYPE OF REPORT & PERIOD COVERED 6. PERFORMING ORG. REPORT NUMBER
7. AUTHOR(s): F. Bozso, J. T. Yates, Jr., W. J. Choyke and L. Muehlhoff		8. CONTRACT OR GRANT NUMBER(s): NR 629-803
9. PERFORMING ORGANIZATION NAME AND ADDRESS: Surface Science Center, Chemistry Department, University of Pittsburgh, Pittsburgh, PA 15260		10. PROGRAM ELEMENT, PROJECT, TASK AREA & WORK UNIT NUMBERS
11. CONTROLLING OFFICE NAME AND ADDRESS		12. REPORT DATE: September 1984 13. NUMBER OF PAGES
14. MONITORING AGENCY NAME & ADDRESS(if different from Controlling Office)		15. SECURITY CLASS. (of this report) 15a. DECLASSIFICATION/DOWNGRADING SCHEDULE

16. DISTRIBUTION STATEMENT (of this Report)

17. DISTRIBUTION STATEMENT (of the abstract entered in Block 20, if different from Report)

18. SUPPLEMENTARY NOTES

Submitted to J. of Applied Physics

19. KEY WORDS (Continue on reverse side if necessary and identify by block number)

Silicon Carbide, Chemical Vapor Deposition, Epitaxy, Buffer Layer.

20. ABSTRACT (Continue on reverse side if necessary and identify by block number)

The reaction of Si(100) ~~with C_2H_4 from a mo~~lecular beam source has been studied using X-ray photoelectron spectroscopy, electron energy loss spectroscopy, and Auger spectroscopy. Using these methods, we have studied the kinetics of SiC formation under conditions where no gas phase excitation processes can contribute. At Si(100) temperatures below 940 K, a "Si + C

DD FORM 1 JAN 73 1473 EDITION OF 1 NOV 65 IS OBSOLETE
S/N 0102-014-6601

SECURITY CLASSIFICATION OF THIS PAGE (When Data Entered)

20. ABSTRACT (continued)

alloy" forms on the surface; annealing to higher temperatures produces SiC exhibiting identical electron spectroscopic properties to SiC(0001). By studies of the characteristic bulk and surface plasmon loss features in the SiC thin film, it has been shown that surface aggregation of bulk Si on top of the growing SiC film occurs at T > 940 K. Under optimum SiC growth conditions, C_2H_4 yields about $2x10^{-3}$ SiC units per C_2H_4 surface collision on Si(100). This study demonstrates the unique type of information which may be obtained by using surface science methods for studies of CVD processes.

Studies of SiC Formation on Si(100) by Chemical Vapor Deposition

F. Bozso[a], J. T. Yates, Jr.[a], W. J. Choyke[b,c] and L. Muehlhoff[b]

Surface Science Center
Department of Chemistry
University of Pittsburgh
Pittsburgh, PA 15260

a. Department of Chemistry
b. Department of Physics
c. Westinghouse R & D Center, Pittsburgh, PA

Studies of SiC Formation on Si(100) by Chemical Vapor Deposition

F. Bozso, J. T. Yates, Jr., W. J. Choyke and L. Muehlhoff

Surface Science Center
Department of Chemistry
University of Pittsburgh
Pittsburgh, PA 15260

ABSTRACT

The reaction of Si(100) with C_2H_4 from a molecular beam source has been studied using X-ray photoelectron spectroscopy, electron energy loss spectroscopy, and Auger spectroscopy. Using these methods, we have studied the kinetics of SiC formation under conditions where no gas phase excitation processes can contribute. At Si(100) temperatures below 940 K, a "Si - C alloy" forms on the surface; annealing to higher temperatures produces SiC exhibiting identical electron spectroscopic properties to SiC(0001). By studies of the characteristic bulk and surface plasmon loss features in the SiC thin film, it has been shown that surface aggregation of bulk Si on top of the growing SiC film occurs at T > 940 K. Under optimum SiC growth conditions, C_2H_4 yields about 2×10^{-3} SiC units per C_2H_4 surface collision on Si(100).

Introduction

In the growth of single crystal cubic SiC by chemical vapor deposition, a major obstacle is the large (20%) mismatch between the deposited SiC and the underlying Si substrate(1,2,3). A buffer layer between the Si and SiC however can provide a proper transition and as has been suggested, it may ease the strain between the two lattices, and good quality SiC single crystal growth becomes possible(4,5,6). It has been found that a proper buffer layer can be formed at near 1400°C substrate temperature either by reaction with propane(4) or by sputtering SiC onto the Si surface(7). Under normal CVD growth conditions (high temperature and high pressure), microscopic studies of the mechanism of the buffer layer formation are particularly difficult.

Our intention has been to devise an experimental system and conditions which will allow the study of kinetic and structural aspects of the epitaxial SiC film growth on Si substrates.

In this work we report the first part of our studies carried out under well controlled conditions in a UHV system. A molecular beam technique for supplying reactant C_2H_4 to a heated Si(100) surface is combined with methods of electron spectroscopy to study the surface layer of SiC produced. By using a molecular beam of C_2H_4 at low gas densities we guarantee that practically no intermolecular collisions of species desorbing from the hot Si surface will occur. This procedure therefore eliminates thermally activated gas phase free radical processes thought to occur in certain Si-CVD processes at high pressures(8).

II. Experimental Details

The apparatus shown in Fig. 1 was employed to study the early stages of SiC growth on Si(100). The system contains a Leybold-Heraeus EA-10 electron spectrometer, Mg/Al anode X-ray source, UTI-100C quadrupole mass spectrometer, molecular beam doser employing a capillary array collimator and a calibrated conductance, and an IQP 10/63 broad profile discharge type sputter source. The base pressure in the system prior to experiments was 10^{-10} Torr. By directing a molecular beam of C_2H_4 at the heated Si(100) crystal, a controlled SiC film growth could be achieved. The molecular beam doser allowed us to expose the Si(100) surface to a variable flux of ethylene. The flux in the present experiments was 1.7×10^{16} molecules C_2H_4 sec^{-1} cm^{-2} corresponding to an effective C_2H_4 pressure of 4.4×10^{-5} Torr. During the exposures the Si(100) crystal was held at various constant temperatures. Periodically the beam was interrupted and the crystal was rotated to the electron spectrometer for XPS, AES and ELS measurements.

The crystal was ohmically heated by a thyristor controlled power supply. In order to eliminate the effects of hot metal parts, a crystal mounting procedure (shown in Fig. 2) was devised. The W wires for support and electric contact are enclosed in edge slots on the Si crystal. A W 26%Re : W 3%Re thermocouple is welded to a tantalum sheet spring which is also wedged into an edge slot. This geometry avoids line-of-sight between the crystal front surface and heated metals, permitting the surface chemistry of Si to be studied without interference.

Calibration of the assembly in vacuum at the melting point of NaCl(s) indicated that Si temperatures may be determined at 1100 K to within ± 20 K.

The cleaning of the Si(100) surface before insertion into the UHV system involved the following chemical treatments with thorough rinsing with H_2O between them:

Step A: trichloroethylene rinse;
Step B: acetone rinse;
Step C: isopropyl alcohol rinse;
Step D: HNO_3 : H_2O (1:1), 5 min. 80°C;
Step E: HF (concentrated), 1 min. 25°C;
Step F: H_2O : H_2O_2 : NH_4OH (5:1:1), 15 min. 80°C;
Step G: H_2O : H_2O_2 : HCl (6:1:1), 15 min. 80°C;
Step H: HF (concentrated), 1 min. 25°C.

In the UHV system the sample was cleaned by low angle argon ion sputtering using 600 eV Ar^+. The XPS and AES spectra of the clean and C_2H_4 exposed Si(100) sample are shown in Fig. 3.

III. Results

1. Kinetics of Carbon Deposition.

The carbon deposition rate, indicative of the growth rate of SiC on Si(100) from C_2H_4 reactant has been studied as a function of substrate temperature in the range of 890 K - 1140 K, using XPS to monitor the C(1s) intensity. Representative data from these measurements are shown in Fig. 4. It can be seen that the initial carbon deposition rate at various temperatures is nearly the same except for the two highest temperature curves, but the C(1s) signal reaches various plateaus by means of a slightly concave initial growth curve. The maximum growth of C(1s) intensity occurs at 940 K and a reversal of apparent C(1s) growth behavior was observed at higher temperatures. Extrapolated maxima of the

C(1s) XPS signal for infinitely large C_2H_4 exposure at increasing temperatures are shown in Fig. 5. Data discussed later indicates that this behavior is due to increased bulk diffusion of carbon from the surface layer at higher temperatures. Persistence of a strong C(1s) XPS signal even after prolonged argon ion sputtering of the sample of SiC grown by C_2H_4 decomposition indicates that a carbon containing layer of considerable thickness is formed by C_2H_4 decomposition on the Si(100) surface. By using a layer model in which SiC layers are postulated to grow on Si(100) surfaces, the XPS data permit the estimate of the SiC film thickness from the I[C(1s)]/I[Si(2s)] intensity ratios, and also the efficiency per C_2H_4 collision for SiC formation. Calculated results based on electron mean free paths(9) of $\lambda^{Si}_{Si(2s)}$ = 30Å, $\lambda^{SiC}_{Si(2s)}$ = 25Å, and $\lambda^{SiC}_{C(1s)}$ = 23Å for the Si(2s) and C(1s) photoelectrons in Si and SiC respectively, are shown in Fig. 6. The carbon to silicon XPS intensity ratio is given by

$$\frac{I[C(1s)]}{I[Si(2s)]} = I^{SiC}_{C} \Big/ \left[I^{SiC}_{Si} + I^{Si}_{Si} \right]$$

where the numerator is the carbon signal from the SiC layer, and the denominator is the sum of the silicon signal from the underlying Si substrate and from the SiC film on top of it. The individual terms in the expression are given by:

$$I_C^{SiC} = \sigma_C N_C^{SiC} \sum_{i=0}^{n-1} \exp - (2i)d_{SiC}/\lambda_C^{SiC} \quad (1)$$

$$I_{Si}^{SiC} = \sigma_{Si} N_{Si}^{SiC} \sum_{j=0}^{n-1} \exp - (2j+1)d_{SiC}/\lambda_{Si}^{SiC} \quad (2)$$

$$I_{Si}^{Si} = \sigma_{Si} N_{Si}^{Si} \sum_{k=0}^{\infty} \exp - (k)d_{Si}/\lambda_{Si}^{Si} \cdot \exp - (2n)d_{SiC}/\lambda_{Si}^{SiC} \quad (3)$$

where σ is the ionization cross section for the 1486.6 eV Al-K_α photons, λ is the electron mean free path, N is the number of C or Si atoms in a 1 cm^2 layer, and d is the interlayer distance in Si and SiC respectively. The numerical mean free path values used are shown in Table I. The second exponential term in equation 3 accounts for the attenuation of the Si(2s) signal of the substrate by the SiC overlayer.

From the calculated SiC thickness versus C_2H_4 dose, the efficiency of the SiC formation in the first ~ 25Å layer was estimated as ~ 10^{-3} SiC units per C_2H_4 surface collision on Si(100) at 940 K. This efficiency is 10^2 - 10^3 times higher than that achieved in conventional CVD processing with C_3H_6 at temperatures near 1650 K(4). The observation of a reduced C(1s) signal above 940 K strongly suggests however that the accumulation of the carbon in the surface layer probed by XPS is influenced by surface-to-bulk and bulk-to-surface diffusion of carbon and silicon respectively.

Table I.

Mean Free Path in Si, λ^{Si} (E) (Å)

Reference	Theory T / Experiment E	Electron Energy (eV) 1400	1380	1330	1200	1150	1100	1000
a	T		20	19.8		18.3	17.9	
b	T		25.9			22.5		
c	T	25.7			22.7			19.6
d	T		27			23		
e	T		30.7	29.9		26.8	25.9	
f	E		27±6	27±6				
g	E		26±2			23±2		

Mean Free Path in SiC, λ^{SiC} (E) (Å)

a	T		35.6	35.2		32.5	31.8	
e	T		25.5	25		22.2	21.5	

2. Study of the SiC Formation on Si(100) by Observation of Plasmon Loss Features.

The plasmon excitation by the X-ray photoemission process or by external electrons (ELS) in Si and SiC has been very valuable in probing the developments of carbon deposition and SiC formation in the surface region of Si(100). In Fig. 7 ELS and XPS spectra of Si(100) and SiC exhibiting strong plasmon loss features are shown. Intense plasmon loss peaks are discernible at 17 eV and 22.5 eV below the Si(2s) XPS and the elastic ELS peak for Si and SiC respectively. The 17 eV and 22.5 eV loss peaks correspond to the well-known Si, and SiC bulk plasmon excitation(10,11,12,13). We have previously characterized the 22.5 eV plasmon loss of SiC by studies of the XPS and ELS spectra of bulk SiC(0001)(14). The 17 eV Si ELS plasmon loss peak exhibits a shoulder at ~ 10 eV which is assigned to the Si surface plasmon excitation(10). It was observed that the plasmon loss peak accompanying the Si(2s) XPS peak was much more intense than the similar ELS peak. That is an indication of intrinsic plasmon excitation in the photoemission process compared to the extrinsic mechanism of the excitation by similar kinetic energy external electrons in ELS.

The basic difference between the plasmon loss components of the electron spectra of Si and SiC provided a tool to probe the structural transformation of the Si surface layer during the CVD process under different conditions.

Kinetic data indicated that at lower temperatures (T < 940K) a smaller, limited amount of carbon could be deposited probably

as a result of diffusion limited growth of the SiC surface layer. The limited lattice mobility in this temperature range may actually prevent the formation of the crystalline SiC. This expectation was supported by the plasmon loss feature of the sample exposed to C_2H_4 at 920 K. ELS spectra with 200 eV and 1400 eV electrons are shown in Fig. 8 following the C_2H_4 exposure and also after subsequent annealing at 1100 K. With 200 eV electrons (probing the near surface region) for the C_2H_4 exposed surface, a broad loss peak was observed centered at ~ 20 eV compared to the 17 eV and 22.3 eV plasmon losses for Si and SiC respectively. With 1400 eV electrons (probing deeper layers below the surface) only the 17 eV Si plasmon loss was discernible, indicating the presence of the underlying Si substrate, and the limited penetration depth of the carbon into the Si substrate at 920 K.

There was a dramatic change in the plasmon loss feature after annealing the surface at 1100 K. With 200 eV electrons the characteristic Si bulk and surface plasmon losses reappeared at 17 eV and ~ 10 eV. With 1400 eV electrons, in addition to the 17 eV peak, a shoulder at 22.5 eV, characteristic of deeper lying SiC was apparent. Based on these observations it can be concluded that at temperatures below about 940 K the carbon deposition on Si(100) did not result in SiC formation. Instead, a Si-C alloy seems to be formed. The deposited carbon in the Si-C alloy however could be converted into SiC by annealing at higher temperatures.

At temperatures near 940 K we can produce SiC layers, and in fact, judging from Figs. 4 and 5, the growth rate of the C(1s) XPS feature is maximized near this temperature. This is demonstrated by the data shown in Fig. 9, for layers produced at 940 K. The evolution of the plasmon loss feature accompanying the C(1s) and Si(2s) XPS peaks as a function of C_2H_4 exposure at 940 K is shown in Fig. 9. With increasing exposure the plasmon loss peak 17 eV below the Si(2s) peak is gradually shifted to 22.5 eV, characteristic for SiC. The plasmon loss peak accompanying the C(1s) peak however occurs at 22.5 eV in the whole exposure range. This behavior of the C(1s) plasmon loss can be explained by the presence of intrinsic loss processes characteristic of Si-C bonding upon core-hole excitation of a C atom in a Si environment. After saturation with C_2H_4 exposure the Si(2s) XPS peak with its plasmon loss features was identical to that of a bulk SiC single crystal, as shown in Fig. 10.

The plasmon loss feature measured by ELS during excitation by electrons in the 100 - 1400 eV energy range indicated interesting details, as shown in Fig. 11. Reducing the electron kinetic energy from 1400 eV to 100 eV the electron penetration/escape depth and hence the layer thickness probed, decreases from ~ 25Å to ~ 6Å(9a). In the case of clean Si(100), as expected, a single plasmon loss peak at 17 eV due to the Si bulk plasmon excitation can be observed in the whole electron kinetic energy range. However, by comparing the 100 eV loss profile to those taken at higher electron energy, a shoulder is seen at ~ 10 eV for the Si(100) surface due to the Si surface plasmon.

A very interesting and unexpected result was obtained upon study of the plasmon loss features present in the SiC film grown on Si(100). In the case of the C_2H_4 exposed Si(100) surface studied with 1400 eV electrons, the plasmon loss feature characteristic of the SiC plasmon loss at 22.5 eV is discernible as expected. With decreasing electron kinetic energy however, a gradual shift of the loss peak from 22.5 eV to 17 eV was observed. In addition to the 17 eV loss peak with 100 eV or lower kinetic energy, even the Si surface plasmon loss at ~ 10 eV could be observed as a shoulder in Fig. 11 and could be more clearly observed under higher resolution.

This observation indicated that the epitaxial SiC layer on Si(100) extends to at least 25Å depth. On the other hand, the presence of Si bulk and surface plasmon losses in experiments probing the near surface layers with lower energy electrons, indicates that the epitaxial SiC film is covered by a Si surface layer. This is a surprising finding which may be of major importance in the processes associated with the production of epitaxial SiC thin films on Si(100).

Discussion

A. Control of SiC Formation - Kinetic Factors.

The growth rate of SiC on Si(100) from C_2H_4 reactant has been studied in the temperature range of 890 K - 1140 K. The kinetic data for SiC formation (Figs. 4 and 5) indicate three distinct temperature ranges, $T < 940$ K, $T \approx 940$ K and $T > 940$ K. In these three temperature ranges the relation between the carbon

supply (r_s) and the carbon bulk diffusion rate (r_d) are $r_s > r_d$, $r_s \approx r_d$ and $r_s < r_d$ respectively. The existence of carbon bulk diffusion in Si and its dramatic effect is clearly shown by the reduced rate of increase of I[C(1s)] with the C_2H_4 exposure at temperatures above 940 K.

The decrease in the rate of growth of I[C(1s)] above 940 K could be due to a decrease in the rate of the chemical reaction of C_2H_4 (g) with Si(100) as the temperature is raised. This would yield a negative temperature coefficient, and could be due, for example, to a temperature-dependent decrease in C_2H_4 sticking coefficient. We have performed an experiment which excludes this explanation as shown in Figure 12. Curve (a) shows the I[C(1s)] signal increase with C_2H_4 exposure at a constant temperature of 1140 K. Curve (b) represents a different experiment with each subsequent C_2H_4 exposure performed at increased temperatures from 890 K to 1140 K. It can be seen that along curve (b) the curvature and slope remain <u>positive</u> throughout the entire temperature range, thereby exluding a negative temperature coefficient as being responsible for the decrease in the rate of growth of I[C(1s)] above 940 K. Instead, the differences between curves (a) and (b) in Figure 12 must be attributed to activated bulk diffusion of C into Si(100). An important characteristic of I[C(1s)] and its derivative, $dI[C(1s)]/dN_{C_2H_4}$ above $N_{C_2H_4} = 3 \times 10^{19}$ cm^{-2} is that these quantities are both larger for curve (b) than curve (a). This implies that the carbon diffusion rate is influenced not only by the temperature but by the thickness and quality of the previously (at lower temperatures) formed SiC

film as well. It is found that Si(100) crystals which, after C_2H_4 exposure have reached the plateau of the I[C(1s)] curve at T < 940 K (see Figure 4), could be annealed at 1140 K for a long time without indication of significant carbon loss from the surface layer by bulk diffusion. In contrast to this it is apparent that during the isothermal exposure to C_2H_4 at 1140 K, a high carbon diffusion rate prevents the buildup of a critical carbon concentration in the surface layer, and at 1140 K a barrier layer for diffusion is not easily formed. However, such a surface barrier layer can be formed at lower temperatures. As shown in Figure 4 and Figure 12, the nearly identical initial slopes of the I[C(1s)] curves indicate that at lower temperatures the overall rate of carbon deposition on Si(100) is not significantly temperature dependent, implying that the C_2H_4 decomposition at the Si(100) surface is not the rate determining step. Based on some known high activation energies of diffusion and self-diffusion, such as ~ 7.2 eV for C and Si self-diffusion in α-SiC(15) and 5 eV for Si self-diffusion in silicon(16,17), the carbon diffusion rate is probably the rate limiting step at lower temperatures.

A high activation energy for diffusion sets a limit to the film thickness, which may grow on the Si substrate as well. For T < 940 K we may assume that $r_s > r_d$. Under these conditions a critical carbon concentration is established in the surface layer, forming a less penetrable (and perhaps for the C_2H_4 decomposition less active) Si-C alloy film. The film, once formed, even if thin, produces a diffusion barrier for carbon and

silicon and film growth is strongly retarded. This can be seen in the sudden turn into a plateau for the I[C(1s)] curves below 940 K in Figure 4 and in the extrapolated I^{max} [C(1s)] values in Figure 5.

Besides the limited thickness of the films formed at lower temperatures, the plasmon loss feature observed below 940 K indicates the formation of a Si-C alloy instead of silicon-carbide (see Figure 8)(11). By annealing at 1100 K, the Si-C alloy could be converted into silicon-carbide, as indicated by the bulk plasmon energy change from ~ 20 eV to 22.5 eV (see Figure 8). It can be concluded therefore from the data below 940 K that both kinetically and energetically a higher temperature is needed for the SiC film formation.

Based on simple considerations, a temperature for which $r_s \approx r_d$ is likely to be the optimum condition for SiC film growth. This seems to be met at 940 K, where the highest I[C(1s)] growth is observed. Details of the XPS and ELS spectra indicate that this temperature not only provides for an optimum diffusion rate enabling thicker film growth, but also a temperature of 940 K is appropriate for the crystalline SiC formation as well. The film grown at 940 K exhibits the 22.5 eV bulk plasmon energy of SiC. This 940 K - SiC film is indistinguishable in its XPS and ELS spectrum from data obtained from a SiC(0001) single crystal (exposing the Si face) (see Figure 10)(14).

B. Absolute Rate of SiC Formation - C_2H_4 + Si(100).

At 940 K the carbon supply rate by decomposition of C_2H_4 at the Si(100) surface and the diffusion rate seemed to result in an

optimum SiC film growth rate under our experimental conditions. The measured SiC growth rate is ~ 0.06Å sec^{-1} with a C_2H_4 flux of 1.7×10^{16} molecules sec^{-1} cm^{-2} on Si(100) at 940 K. This means that the efficiency of SiC formation per C_2H_4 surface collision (at an effective C_2H_4 pressure of 4.4×10^{-5} Torr) is two orders of magnitude greater than achieved in conventional CVD processing near 1600 K and in the 1 Torr hydrocarbon pressure range.

C. Layer Structure in SiC/Si(100) Film Formation.

We have found that a surprising and unexpected feature is involved in SiC formation on Si(100). Under conditions of optimal SiC film growth, the SiC layer is covered by a few layers of Si, and this Si surface layer exhibits characteristic Si bulk plasmon (17 eV) and Si surface plasmon (10 eV) energy loss features in the ELS spectra. Thus, a supply of surface Si exists during C_2H_4 reaction with Si(100) even when many atomic layers of SiC have formed.

Silicon surface layers of increasing thickness are observed after higher temperature (T > 940 K) C_2H_4 exposures. This is seen by the observation of more pronounced Si bulk and surface plasmon losses in the ELS spectra at 17 eV and 10 eV for increased electron kinetic energy, i.e., deeper probing depths. The presence of a Si overlayer is confirmed by the comparison of the C(1s) XPS and the C-AES signal intensities after C_2H_4 exposure at increasing temperatures, as shown in Figure 13. The carbon XPS signal continuously increases for all reaction temperatures between 890 K and 1140 K while the AES peak-to-peak height goes through a maxima at 990 K as a result of attenuation

by the increasing Si layer thickness on top of the carbon containing layer. The main reason for this behavior is a much larger escape depth of the ~ 1200 eV XPS photoelectrons. Observations of a similar type regarding Si overlayers on thin films have recently been made in the palladium-silicide (Pd_2Si) system(18). The thermodynamic factors responsible for Si segregation to SiC layers are not understood at present.

D. Intrinsic SiC Plasmon Generation in SiC.

The plasmon satellites occurring on the low energy side of the XPS peaks may be of extrinsic or intrinsic origin associated with collective valence electron density oscillation generated by the fast moving photoelectrons (extrinsic) or by the ionization event itself (intrinsic)(19-21). The distinction between the two plasmon excitation mechanisms has long been a subject of study and discussion (21-29). The plasmon loss features of the XPS and ELS spectra in this work support the primary intrinsic mechanism of plasmon excitation in SiC.

The first of two indications of an intrinsic plasmon excitation process is that the peak ratio of the first plasmon loss peak to the main XPS peak is a factor of three or more higher than that of the first loss peak to the elastic peak in ELS experiments (involving a similar electron kinetic energy). Since the average path length in the sample is the same for X-ray photoelectrons and external electrons of the same kinetic energy, the higher peak ratio for the X-ray excited plasmons indicates the contribution of a different excitation mechanism that is an intrinsic plasmon excitation mechanism.

The second indication of an intrinsic excitation mechanism is that for lower surface layer carbon concentrations still silicon rich and far short of extended SiC film formation, the plasmon loss peak to C(1s) XPS peak separation is 22.5 eV, equal to the bulk plasmon energy of SiC while the separation from the Si(2s) peak is 17 eV, characteristic of bulk silicon (see Figure 7). Should the C(1s) photoelectrons excite plasmons extrinsically while they are passing through the media, they would excite with equal or even higher probability Si bulk plasmons. Since the 22.5 eV plasmon is observed, a prevailing intrinsic excitation mechanism is likely. A second important assumption may be based on the observed 22.5 eV plasmon energy in the low carbon concentration samples namely that the valence electron density oscillation seems to be very local, possibly involving only a few or maybe just one elementary cell of the solid.

E. Summary of Results.

The results of this study are summarized below:

1. The reaction of Si(100) with C_2H_4 to produce a Si - C alloy is observed at temperatures in the range of 890 - 940 K. This reaction is a surface reaction, independent of gas phase excitation processes.

2. At a Si(100) temperature of 940 K, diffusion processes in the bulk begin to dominate the kinetics of the surface reaction process and SiC begins to form, yielding the characteristic 22.5 eV SiC plasmon loss.

3. At a Si(100) temperature of 940 K and above, surface segregation of bulk Si is observed on the growing SiC layer.

4. The efficiency of SiC formation at 940 K is approximately 2×10^{-3} per C_2H_4 collision with the Si(100) surface.

5. The three temperature regions for film growth are schematically summarized in Figure 14. At 850 K $<$ T $<$ 940 K, $r_s > r_d$ and a thin Si-C alloy film growth is observed. At T $\cong$ 940 K, $r_s \cong r_d$, and a thick SiC film is formed along with a bulk Si overlayer. At T > 1000K, $r_s < r_d$, and carbon bulk diffusion dominates, along with SiC formation and a Si overlayer formation.

IV. Acknowledgments

We acknowledge with thanks, support of this work by the Office of Naval Research under Contract No. SFRCN00014-82-K-0280.

FIGURE CAPTIONS

Figure 1. Apparatus.

Figure 2. Crystal Mounting.

Figure 3. XPS and AES - clean and C_2H_4 exposed Si(100).

Figure 4. C(1s) intensity versus $N_{C_2H_4}$.

Figure 5. Extrapolated C(1s) plateau intensities.

Figure 6. SiC Thickness (calculated) versus $N_{C_2H_4}$.

Figure 7. Plasmon Loss Features of Si(100) and SiC by EELS and XPS.

Figure 8. Plasmon Behavior of Si(100) Exposed to C_2H_4 at 920 K.

Figure 9. Plasmon Loss Features for Increasing Exposure of Si(100) to C_2H_4 at 940 K.

Figure 10. Comparison of SiC Plasmon Features with SiC/Si(100) Film and with Si(100).

Figure 11. Electron Energy Dependence of Plasmon Loss Features.

Figure 12. Comparison of C(1s) Intensity for Isothermal (1140 K) and for Stepped-Temperature Reaction - Si(100) + C_2H_4.

Figure 13. Comparison of XPS and AES Measurements on Si(100) for Increasing Temperature of SiC Formation.

Figure 14. Three Temperature Ranges of SiC Growth on Si(100) from C_2H_4.

REFERENCES

(1) W. C. Nieberding and J. A. Powell, IEEE Trans. Ind. Electron. 1E-29, (1982) 103.

(2) K. A. Jacobson, J. Electrochem. Soc. 118, (1971) 1001.

(3) K. Kuroiwa and T. Sugano, J. Electrochem. Soc. 120, (1973) 138.

(4) S. Nishino, J. A. Powell and H. A. Will, Appl. Phys. Lett. 42, (1983) 460.

(5) Y. Hamakawa, K. Fujimoto, K. Okuda, Y. Kashima, S. Nonomura and H. Okamoto, Appl. Phys. Lett. 43, (1983) 644.

(6) A. Addamiano and J. A. Sprague, Appl. Phys. Lett. 44, (1984) 525.

(7) S. Nishino, Y. Hazuki, H. Matsumani and T. Tanaka, J. Electrochem. Soc. 127, (1980) 2674.

(8) M. E. Coltrain, R. J. Kee, and J. A. Miller, J. Electrochem. Soc., 131 (1984) 425.

(9a) M. P. Seah and W. A. Dench, Surf. Interface Anal. 1, (1979) 2.

b) Maria F. Ebel and W. Lieble, J. Electron Spectrosc. 16, (1979) 463.

c) David R. Penn, J. Electron Spectrosc. 9, (1976) 29.

d) F. Bechstedt and K. Hübner, Phys. Status Solidi A 67, (1981) 517.

e) J. Szajman, J. Liesegang, J. G. Jenkin and R.C.G. Leckey, J. Electron Spectrosc. 23, (1981) 97.

f) J. M. Hill, D. G. Royce, M. Mehta, C. S. Fadley, L. F. Wagner, and F. J. Grunther, J. Vac. Sci. Technol. 14, (1977) 376.

g) R. Flitsch and S. I. Raider, J. Vac. Sci. Technol. 12, (1975) 305.

(10) L. I. Johanson and I. Lindau, Solid State Commun. 29, (1979) 379.

(11) Y. Katayama, T. Shimada and K. Usami, Phys. Rev. Lett. 46, (1981) 1146.

(12) T. Ito, M. Iwami and A. Hiraki, Solid State Commun. 36, (1980) 695.

(13) J. H. Thomas III and S. Hofman, Surf. Interface Anal. 4, (1982) 157.

(14) F. Bozso, L. Muehlhoff, M. Trenary, W. J. Choyke and J. T. Yates, Jr., J. Vac. Sci. Technol. (in press).

(15) J. D. Hong, R. F. Davis and D. E. Newbury, J. Mater. Sci. 16, (1981) 2765.

(16) R. N. Ghoshtagore, Phys. Rev. Lett. 16, (1966) 890.

(17) M. Osino, Y. Oana and M. Watanabe, Phys. Status Solidi A72, (1982) 535.

(18) P. S. Ho, P. E. Schmid and H. Föll, Phys. Rev. Lett. 46, (1981) 782.

(19) D. C. Langreth, Nobel 24, (1973) 210.

(20) A. M. Bradshaw, W. Domcke and L. S. Cederbaum, Phys. Rev. B 16, (1977) 1480.

(21) J. C. Fuggle, J. Electron Spectrosc. 9, (1977) 99.

(22) J. E. Houston and. R. L. Park, Solid State Commun. 10, (1972) 91.

(23) A. M. Bradshaw, S. L. Cederbaum, W. Domcke, and U. Krause, J. Phys. C 7, (1974) 4503.

(24) R. L. Park, J. E. Houston and G. E. Laramore, Jpn. J. Appl. Phys. Suppl. 2, (1974) 757.

(25) R. A. Pollak, L. Ley, F. K. McFeely, S. P. Kowalczyk, and D. A. Shirley, J. Electron Spectrosc. 3, (1974) 381.

(26) A. M. Bradshaw and W. Wyrobisch, J. Electron Spectrosc. 7, (1975) 45.

(27) A. Barrie and F. J. Street, J. Electron Spectrosc. 7, (1975) 1.

(28) W. J. Pardee, G. D. Mahan, D. E. Eastman, R. A. Pollak, L. Ley, F. R. McFeely, S. P. Kowalczyk, and D. A. Shirley, Phys. Rev. B 11, (1975) 3614.

(29) J. C. Fuggle, D. J. Fabian, and L. M. Watson, J. Electron Spectrosc. 9, (1976) 99.

Schematic View of UHV Apparatus for Studies of Semiconductor Surfaces

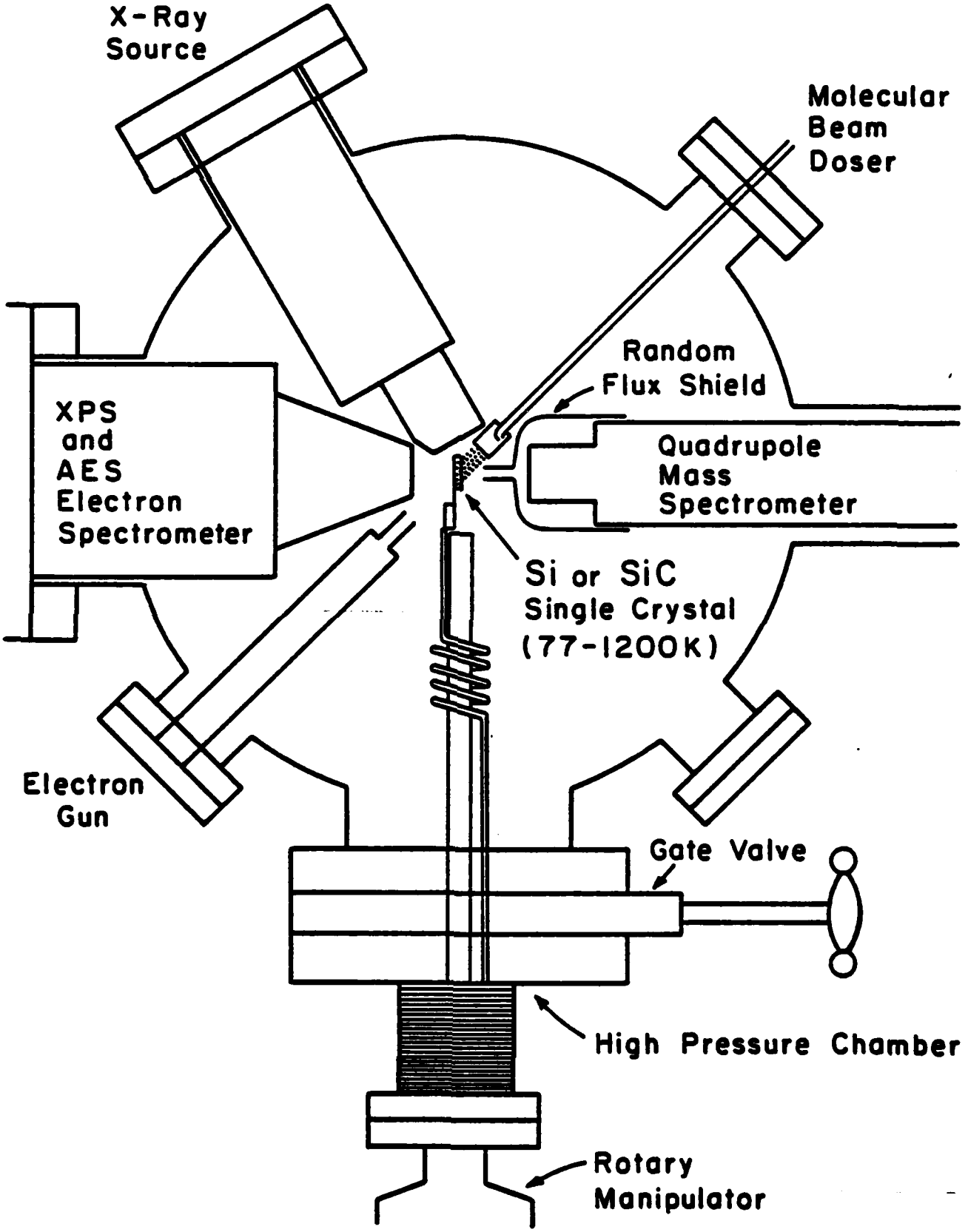

Fig .1

Schematic Diagram of Si Mounting and Heating Method

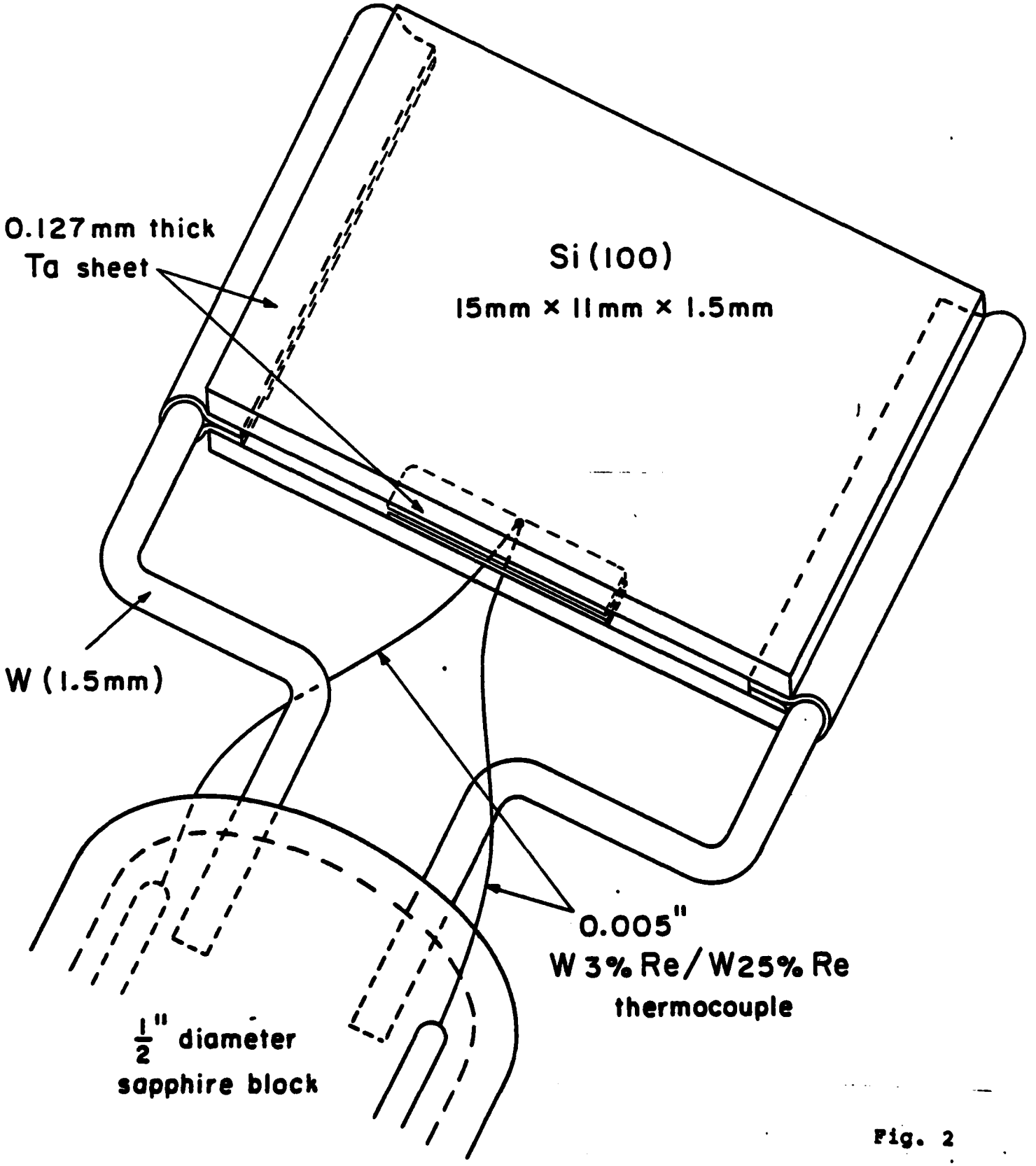

Fig. 2

AES and XPS Spectra of Clean and C_2H_4 Exposed Si(100)

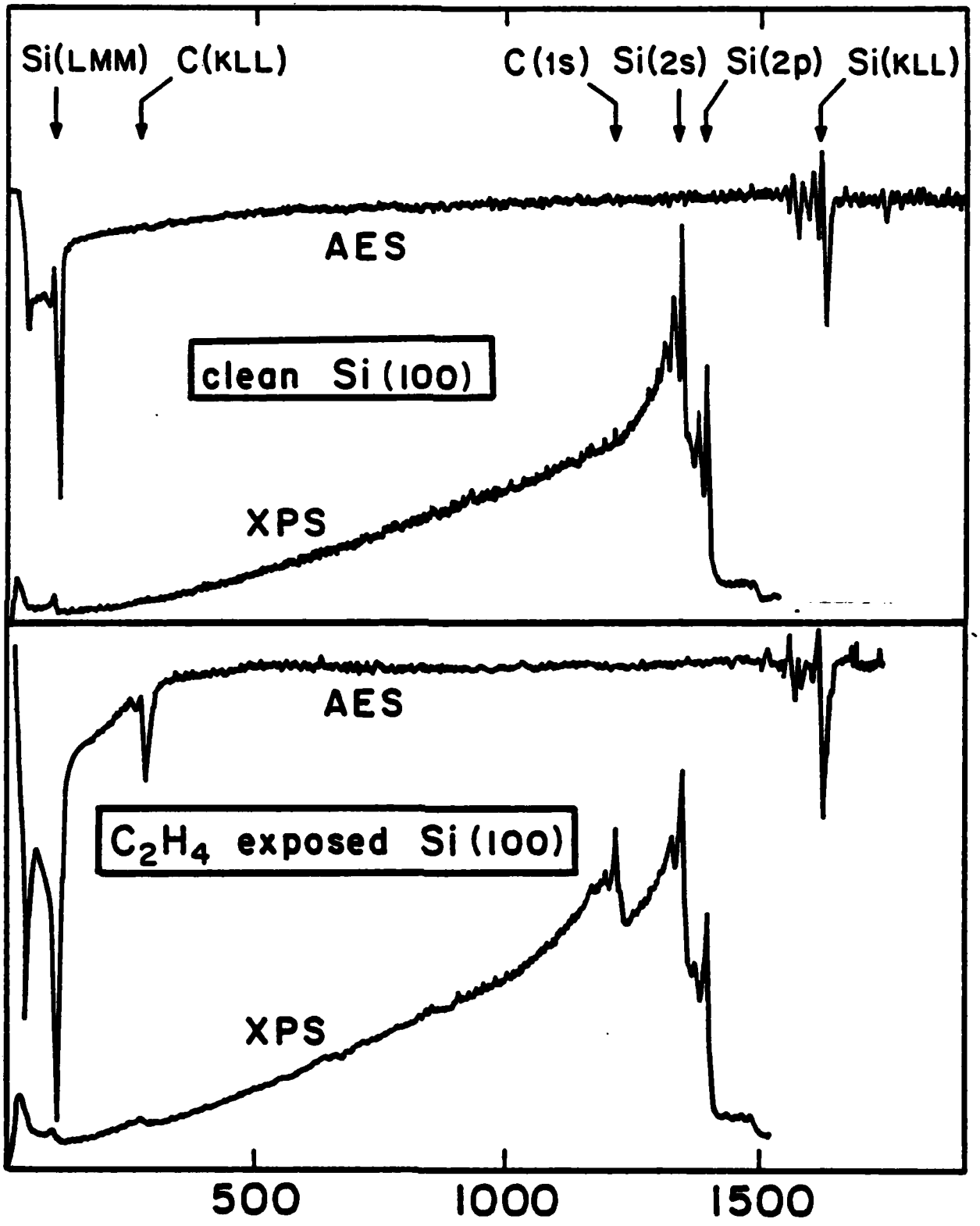

Fig. 3

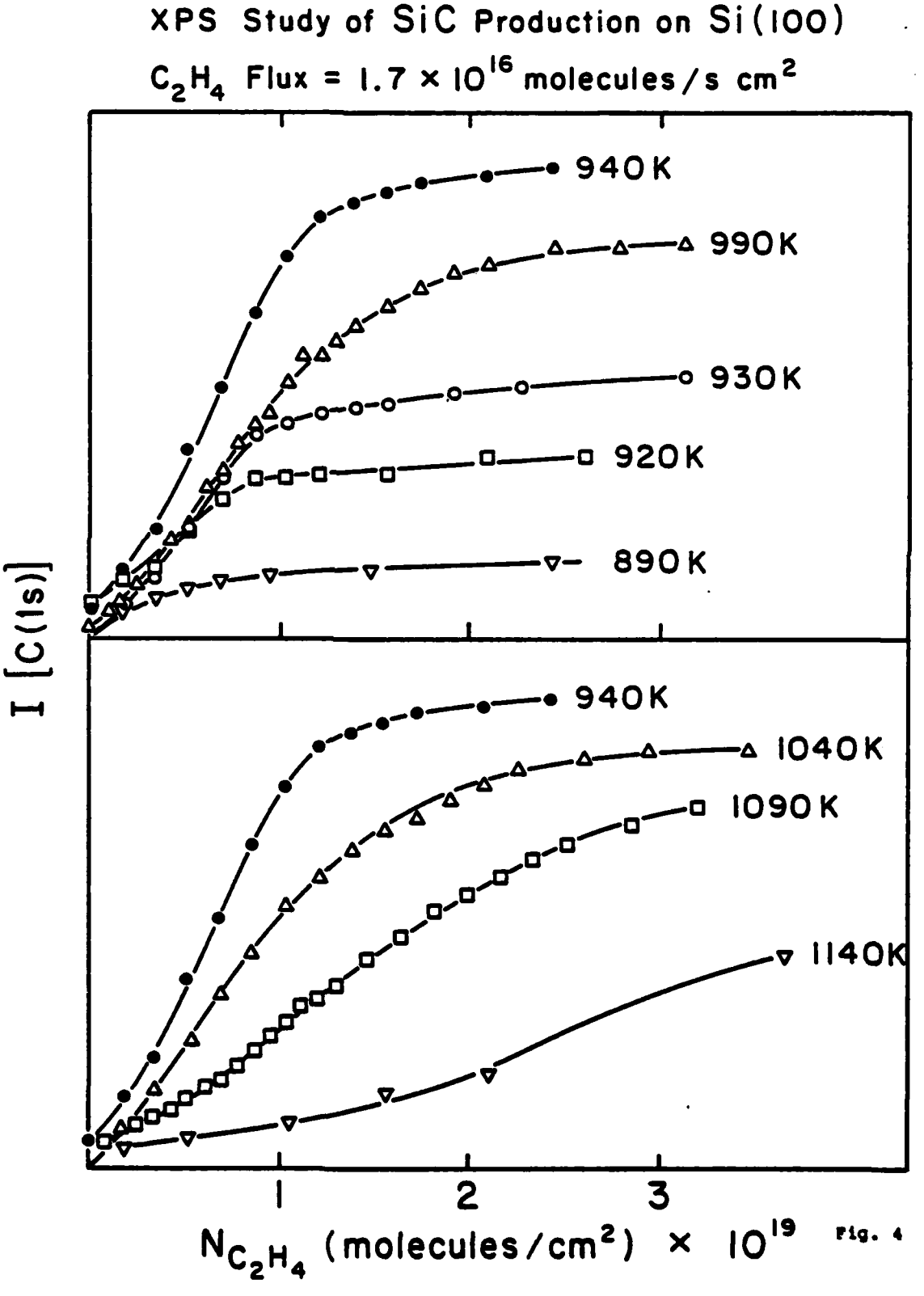
XPS Study of SiC Production on Si(100)
C_2H_4 Flux = 1.7×10^{16} molecules/s cm^2
940K
990K
930K
920K
890K
940K
1040K
1090K
1140K
I [C(1s)]
1
2
3
$N_{C_2H_4}$ (molecules/cm^2) × 10^{19}

Fig. 4

Behavior of C(1s) Maximum Intensity vs. Si(100) Temperature

C_2H_4 Flux = 1.7×10^{16} molecules/s cm^2

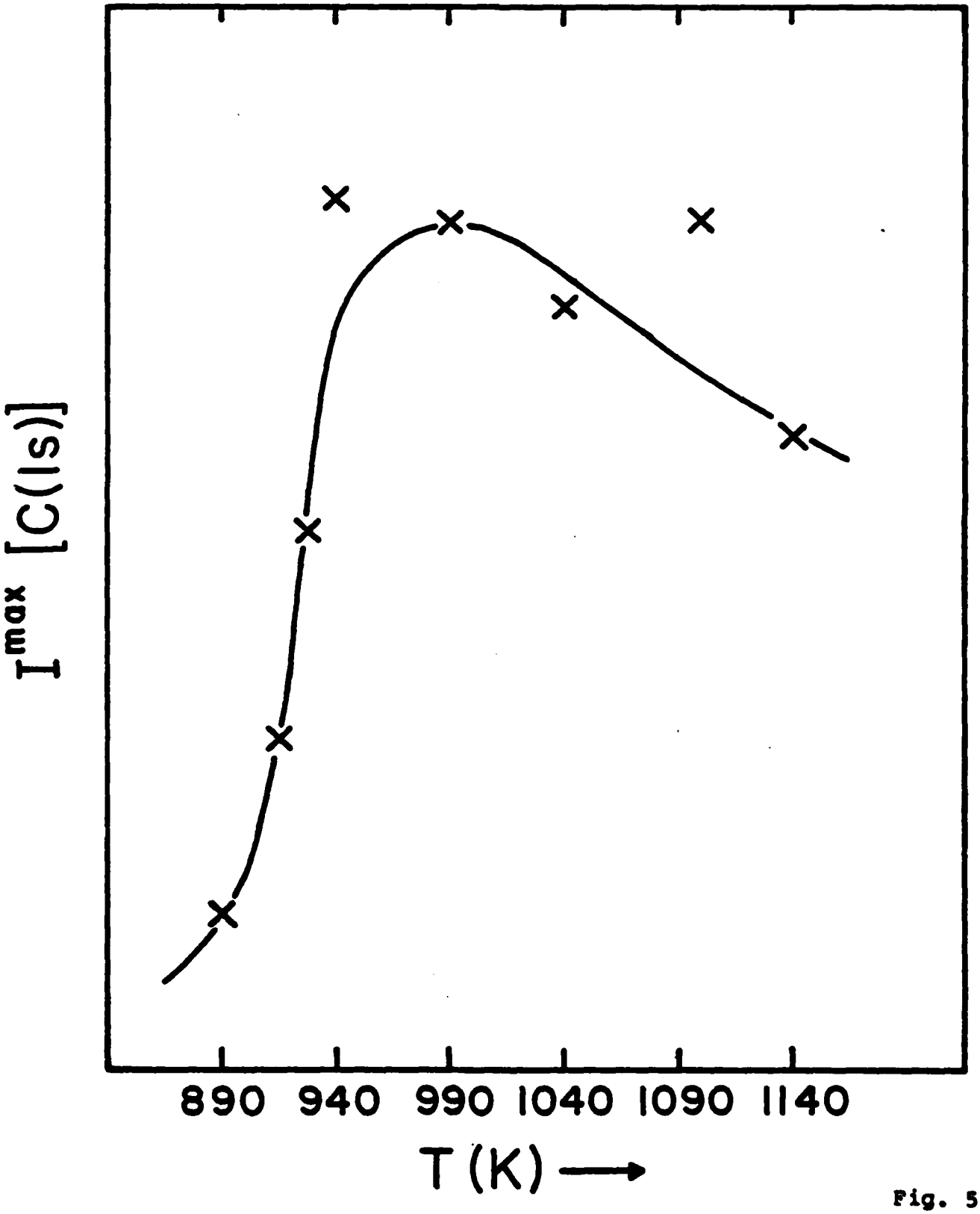

Fig. 5

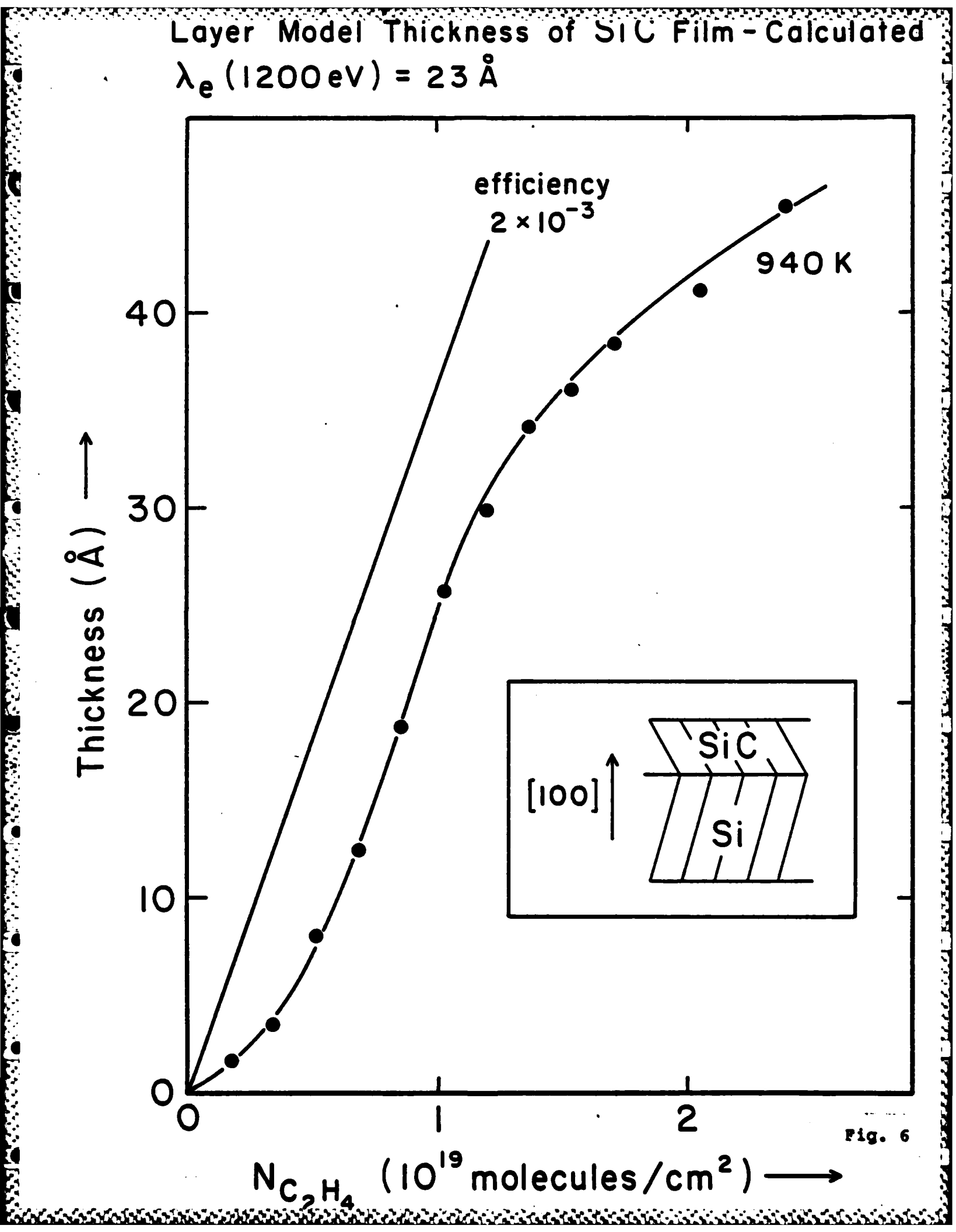
Layer Model Thickness of SiC Film - Calculated
λ_e (1200 eV) = 23 Å
efficiency
2×10^{-3}
940 K
Thickness (Å) ⟶
0
10
20
30
40
0
1
2
$N_{C_2H_4}$ (10^{19} molecules/cm^2) ⟶
[100]
SiC
Si

Fig. 6

Plasmon Loss Features of Si(100) and SiC by Electron Energy Loss and XPS Measurements

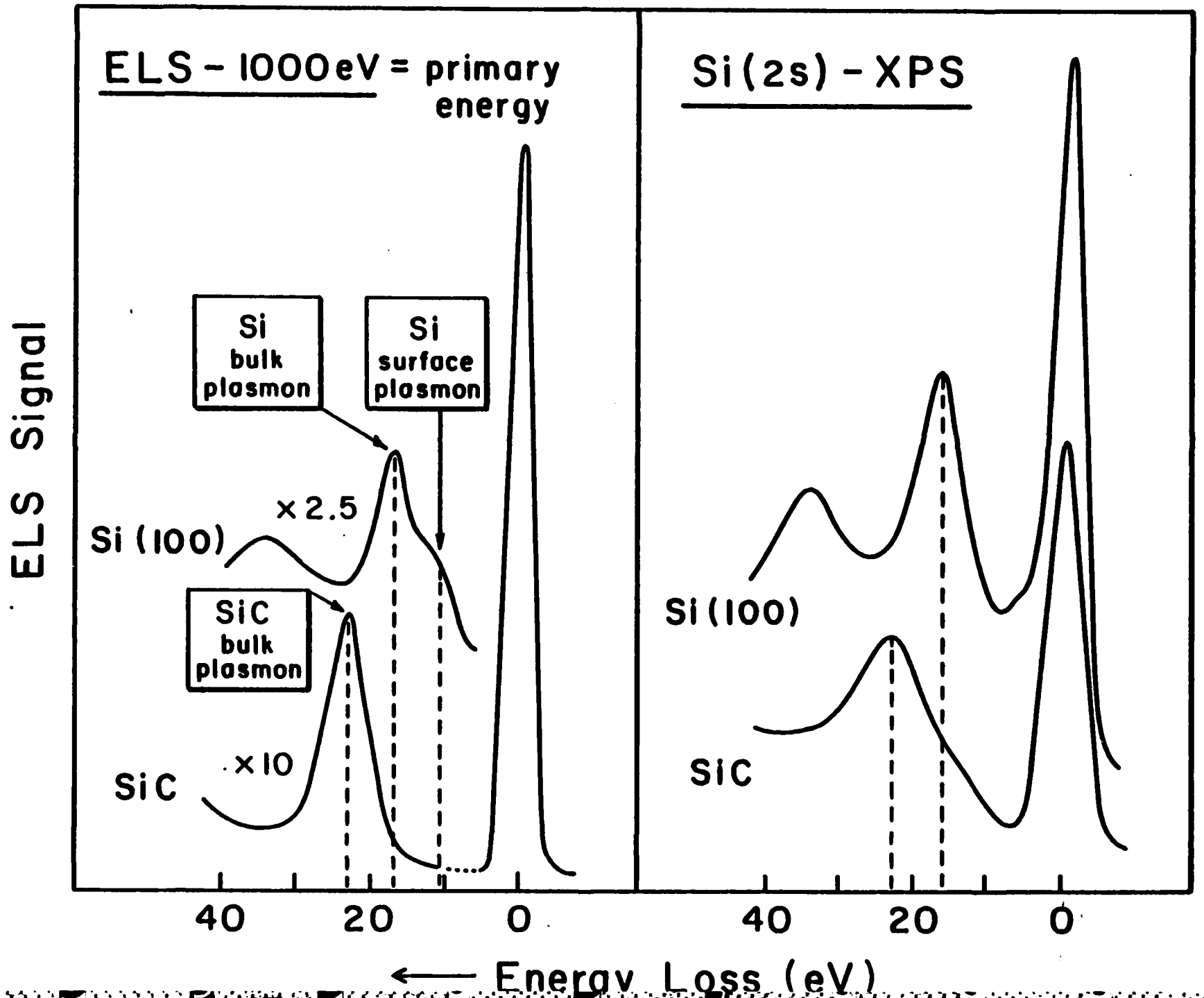

Fig. 7

Plasmon Behavior for Various Treatments of Si(100) to Produce SiC Layer. ELS Measurement.

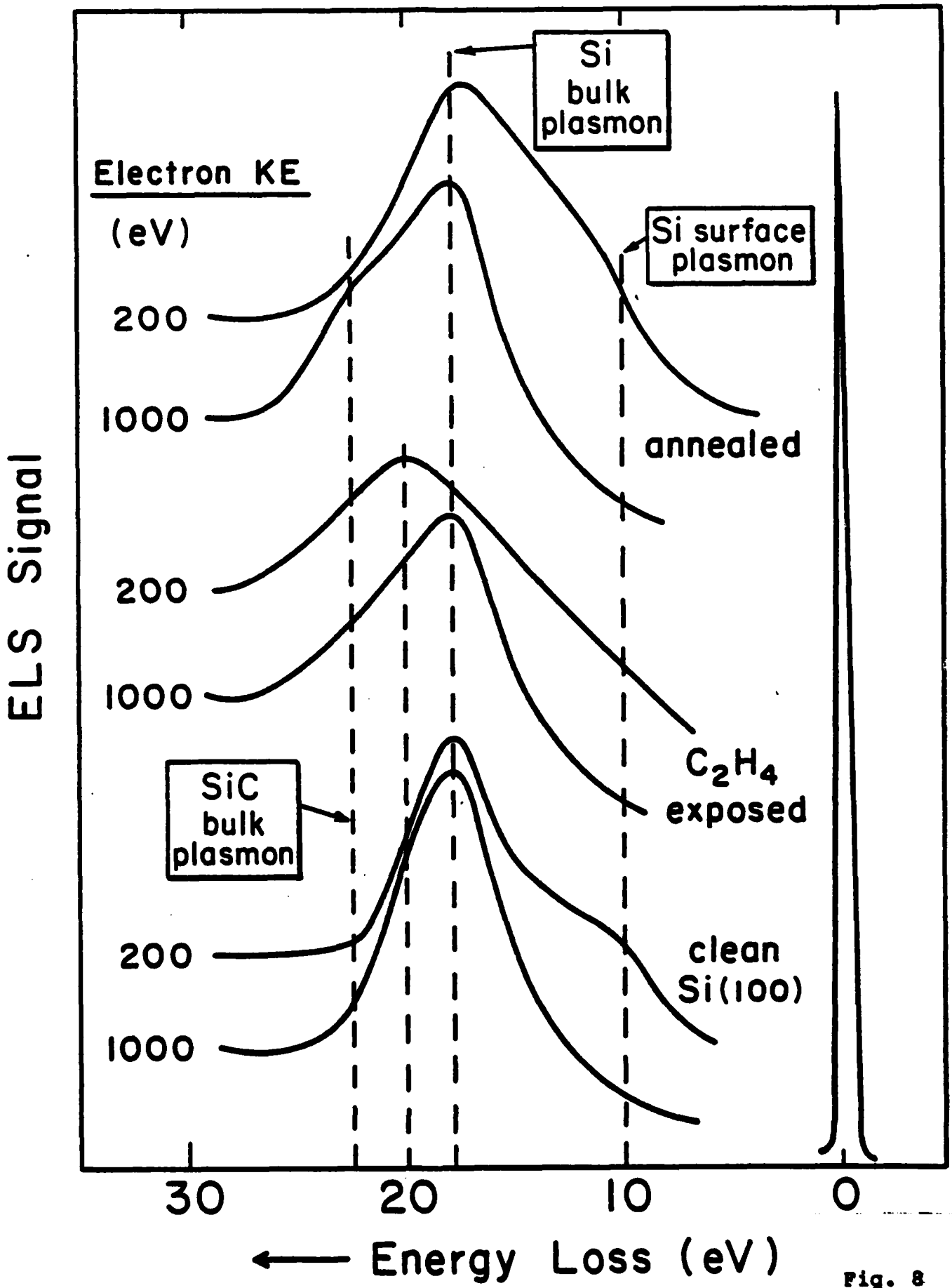

Fig. 8

Plasmon Loss Features for Increasing Exposure of Si(100) to C_2H_4

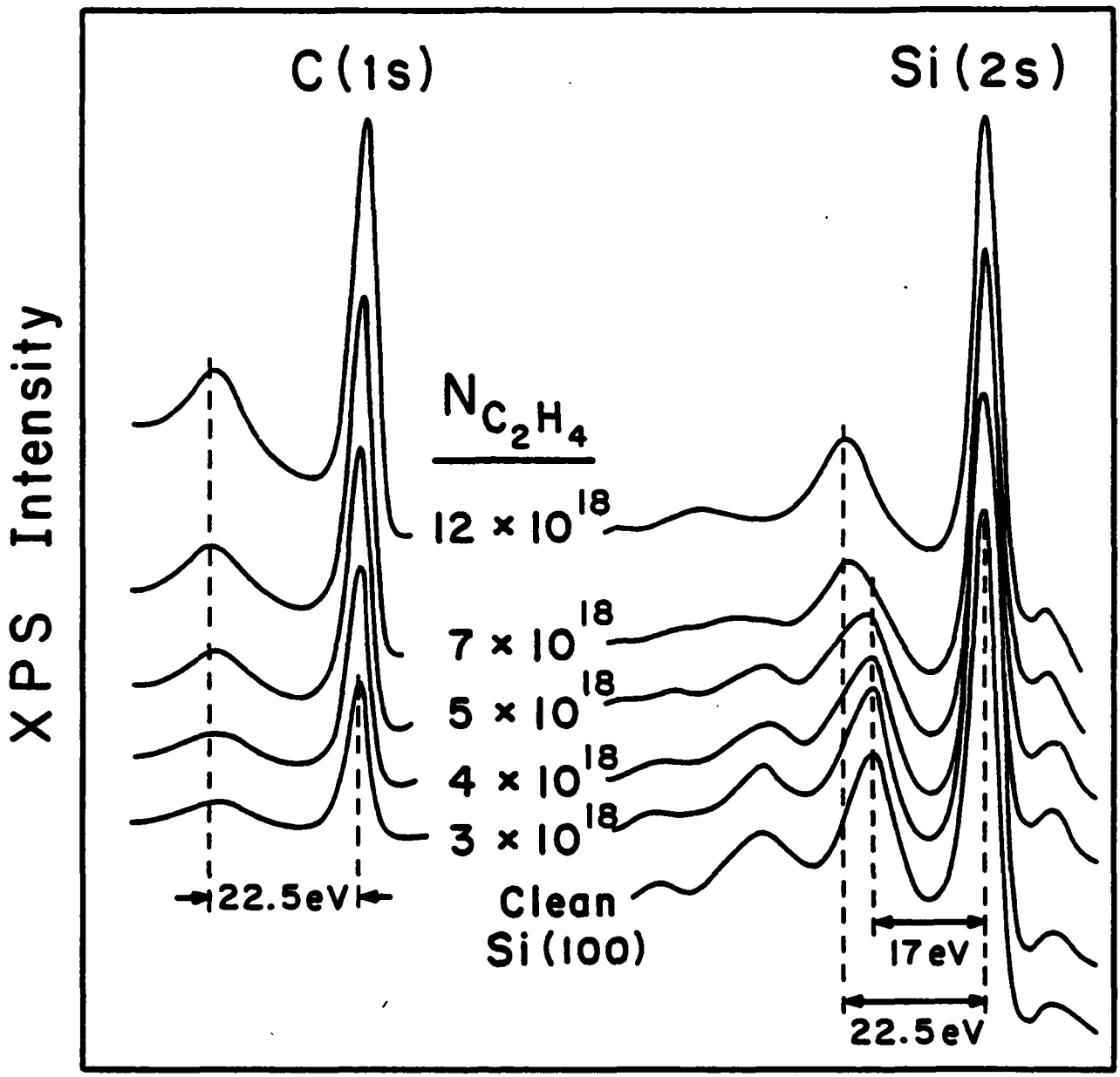

Fig. 9

Comparison of SiC Plasmon Features with SiC/Si(100) Film and with Si(100)

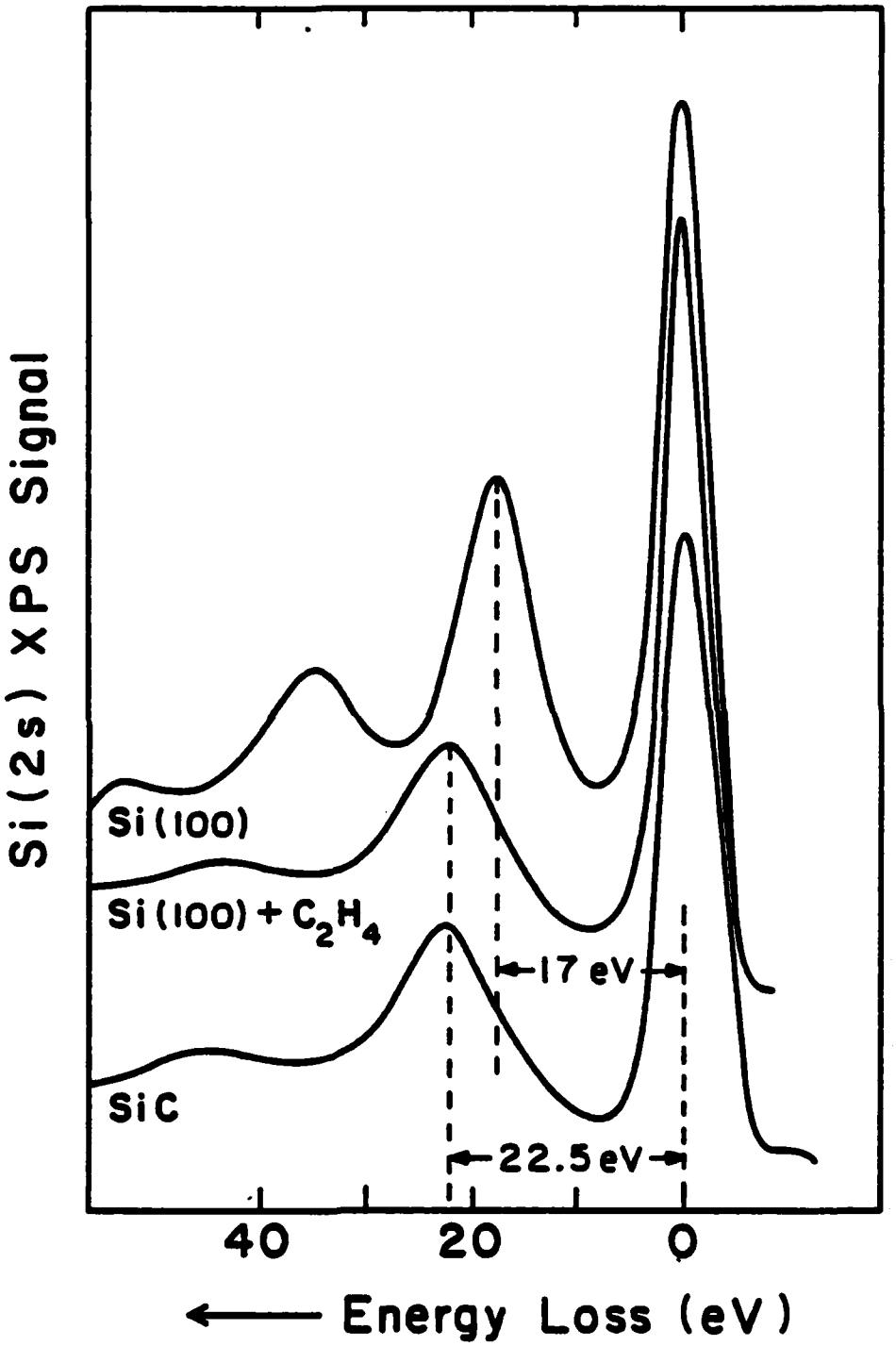

Fig. 10

Fig. 11

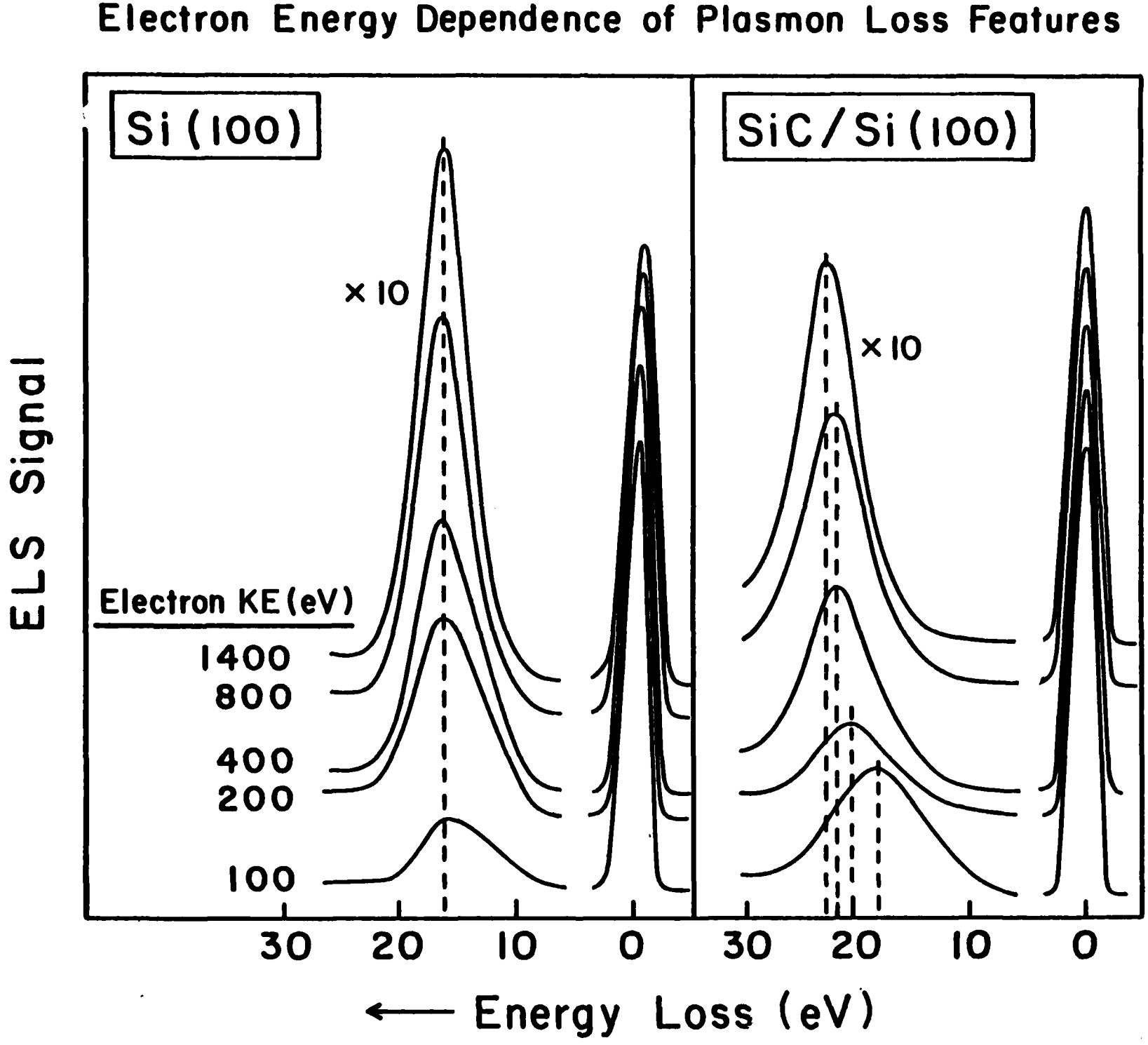
Electron Energy Dependence of Plasmon Loss Features
Si (100)
SiC / Si (100)
× 10
× 10
ELS Signal
Electron KE (eV)
1400
800
400
200
100
30
20
10
0
30
20
10
0
← Energy Loss (eV)

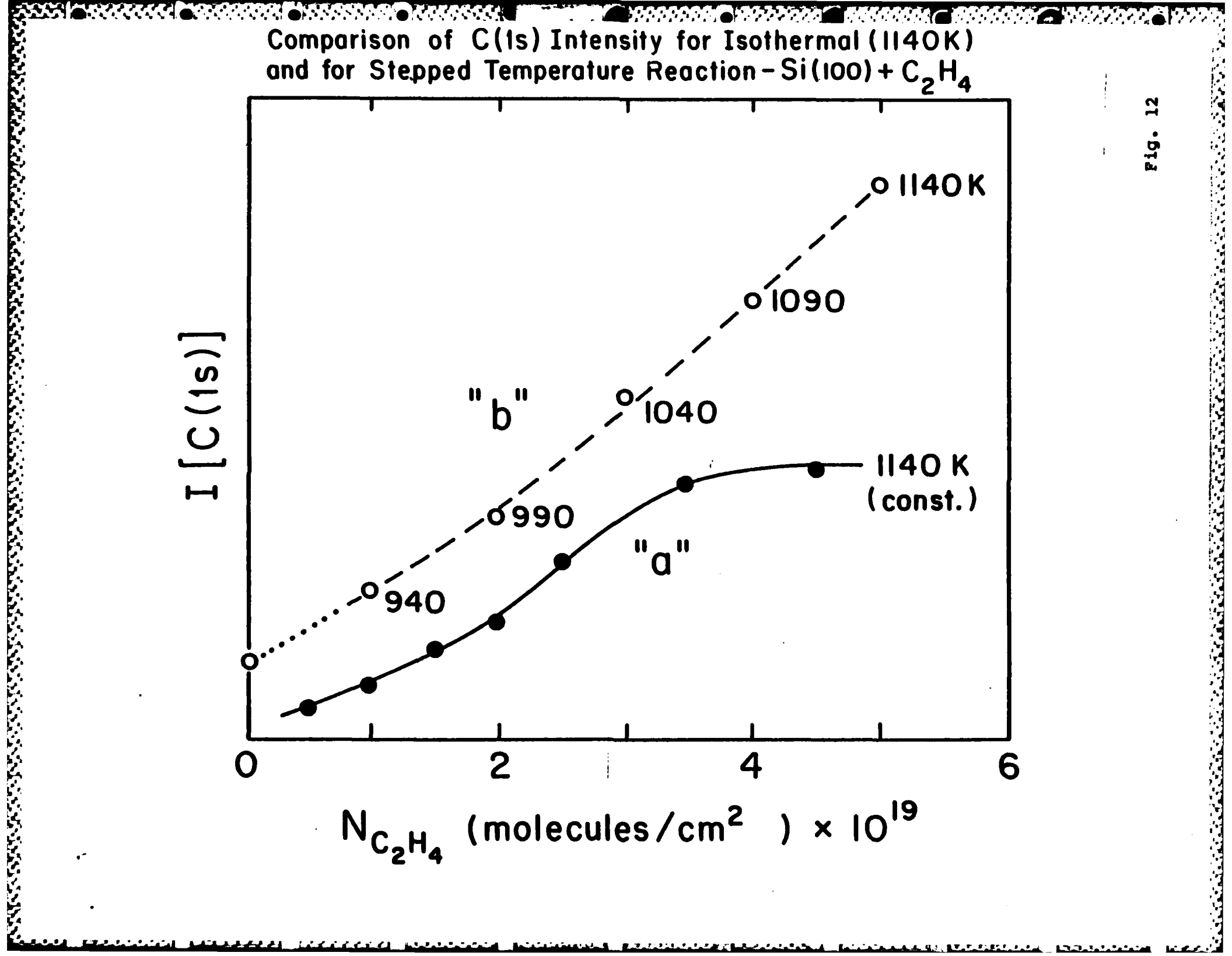
Comparison of C(1s) Intensity for Isothermal (1140K) and for Stepped Temperature Reaction - Si(100) + C_2H_4
I [C(1s)]
1140K
1090
"b"
1040
990
940
1140 K (const.)
"a"
0
2
4
6
$N_{C_2H_4}$ (molecules/cm^2) × 10^{19}

Fig. 12

Comparison of XPS and AES Measurements on Si(100) for Increasing Temperature of SiC Formation

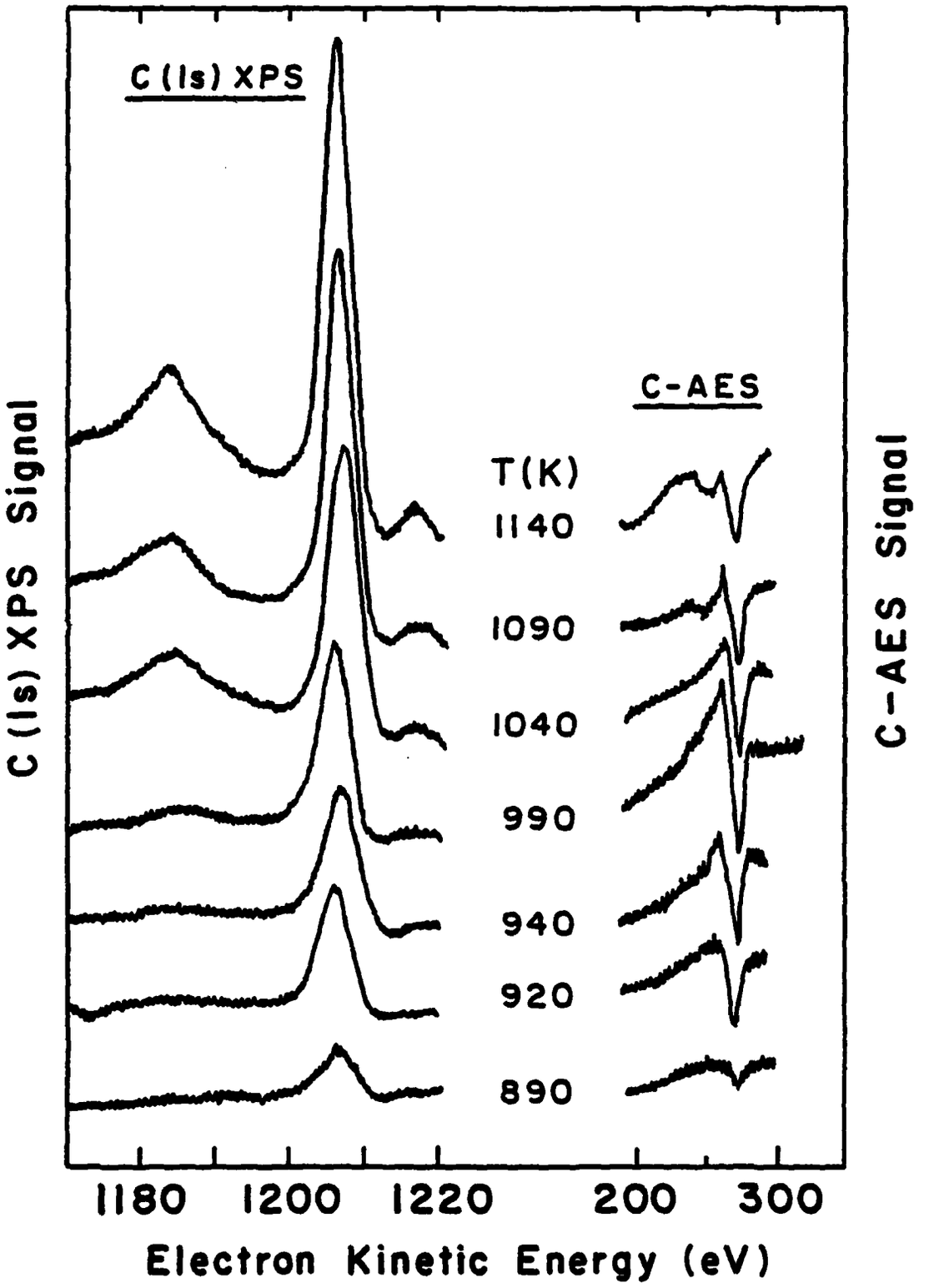

Fig. 13

Three Temperature Ranges of SiC Growth on Si(100) from C_2H_4 - Schematic

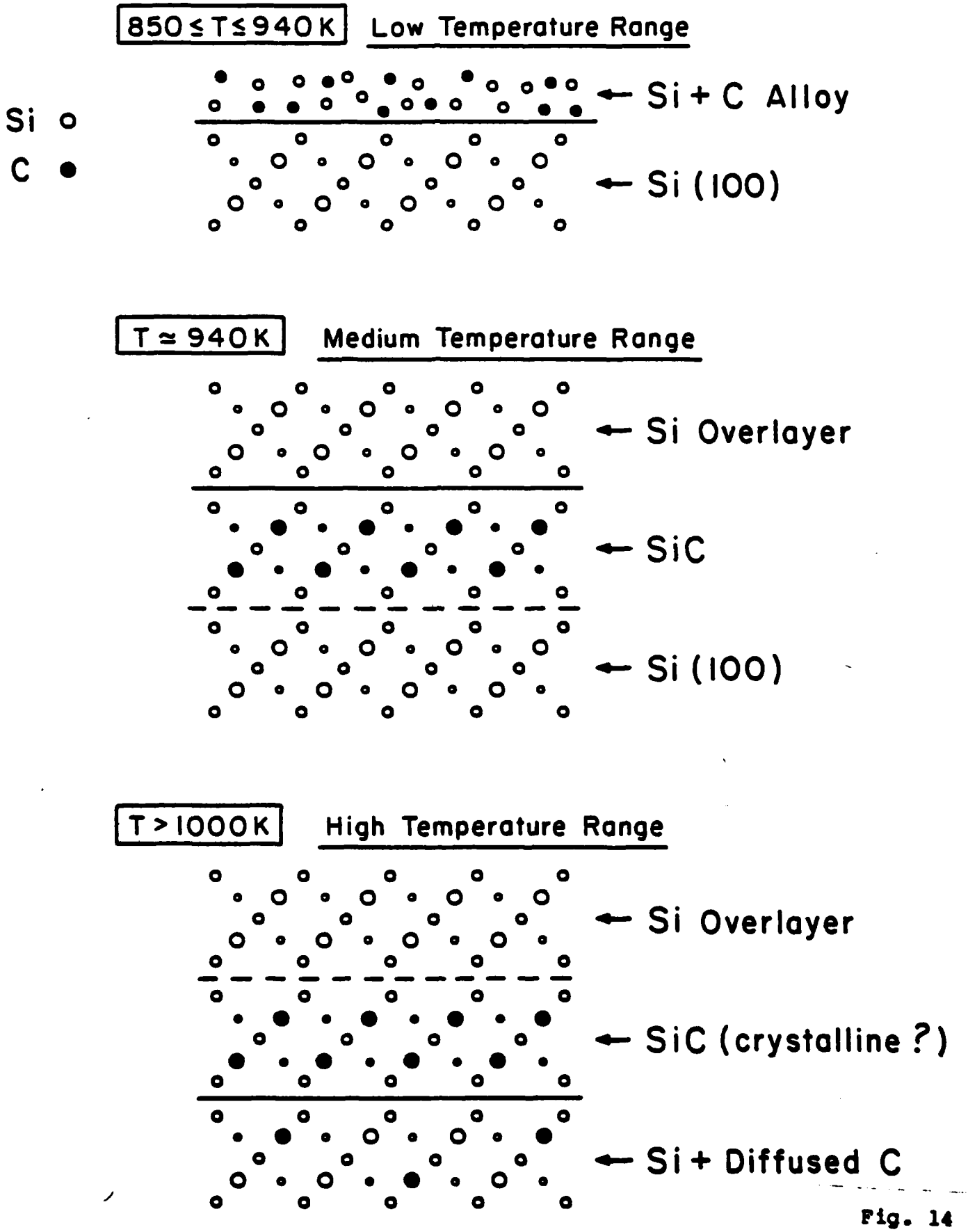

Fig. 14

END

FILMED

11-84

DTIC